13th Deep Sea Offshore Wind R&D Conference, EERA DeepWind'2016, 20-22 January 2016, Trondheim, Norway

Proof of concept for wind turbine wake investigations with the RPAS SUMO

Joachim Reuder[a,*], Line Båserud[a], Stephan Kral[a,b], Valerie Kumer[a], Jan Willem Wagenaar[c], Andreas Knauer[d]

[a]*Geophysical Institute, University of Bergen and Bjerknes Center for Climate Research, Allegaten 70, N-5007 Bergen, Norway*
[b]*Finnish Meteorological Institute, Helsinki, Finland*
[c]*Energy Research Center of the Netherlands (ECN), Westerduinweg 3 1755 LE Petten, The Netherlands*
[d]*Statoil ASA, Bergen, Norway*

Abstract

The Small Unmanned Meteorological Observer (SUMO) has been operated in the vicinity of five research turbines of the Energy Research Centre of the Netherlands (ECN) at the test site Wieringermeer. The intention of the campaign was to proof the capability of the system for wind turbine wake investigations also for situations above rated wind speed. In rather high wind conditions of 15-20 ms^{-1} on May 10, 2014, the system showed a satisfying in-flight behavior and performed five racetrack flights. The racetrack patterns flown parallel to the row of the five turbines (four flights downstream the turbine row, one upstream) enable the characterization and investigation of the strength, i.e. the reduction in the mean wind, and structure, i.e. the horizontal extension and turbulent kinetic energy (TKE) distribution of single turbine wakes.
© 2016 The Authors. Published by Elsevier Ltd.
Peer-review under responsibility of SINTEF Energi AS.

Keywords: wind turbine wake; Remotely Piloted Aircraft System (RPAS); turbulence; turbulent kinetic energy (TKE); NORCOWE; WINTWEX-W;

1. Introduction

The knowledge of the structure and dynamics of single turbine wakes is the key for the understanding of the the wind field inside a wind farm and therefore of major interest and importance for wind farm designers and operators. The wake region of a wind turbine is in general characterized by a reduction of average wind speed and an enhancement of turbulence. By reducing the power output and increasing loads and fatigue for downstream turbines, have both effects negative implications for the operation and maintenance of turbines and wind farms.

In a full-scale perspective have wake investigations during the last years mainly been performed in-situ by mast-based wind profile and turbulence measurements, or by means of sodar [1,2] and lidar remote sensing [3–5]. With

Fig. 1. The left picture shows the SUMO system during the initialization before start. The 5HP for turbulence measurements is the grey tube mounted on the nose of the airframe. The smaller green frame above is a fast-response fine-wire temperature sensor that has been flown for test purposes. The picture on the right shows SUMO in operation in front of two of the NORDEX N80 2.5 MW test turbines. The 108 *m* meteorological mast can be seen in the lower left corner of this picture.

respect to turbulence characteristics, the in-situ measurements from a mast give a good temporal resolution, but are limited to point measurements at the location of an available mast. Remote sensing, in particular by scanning lidar systems, gives flexibility in spatial probing. However, lidars provide per definition volume averages instead of point measurements.

The development and fast growing application of Remotely Piloted Aircraft System (RPAS) in atmospheric science during the last decade [6] opens now up for complementary airborne measurement approaches. First attempts to characterize the flow field and the turbulence structure in the vicinity of wind turbines have been reported [7–9]. However, these studies are either based on a relatively large airframe, e.g. the MASC, developed and operated by the University of Tübingen [7], or on a very advanced but expensive flow probe developed and flown by a group at ETH Zürich [8,9]. After implementing a reasonably priced commercial flow probe [10] in the SUMO system [11], developed and operated by the University of Bergen, this study presents a proof of concept of the capability of this system and is structured as follows. A short description of the SUMO system in Section 2 is followed by a presentation of the measurement campaign and in particular the SUMO operations in Section 3. Section 4 presents and discusses the results before ending with a short summary and outlook in Section 5.

2. The SUMO system

The Small Unmanned Meteorological Observer (SUMO) is a micro-RPAS of about 80 *cm* length and wingspan and a take-off weight of around 650 *g*. It is developed in collaboration between the Geophysical Institute in Bergen and the Lindenberg and Müller GmbH [12]. The system has been subject to numerous improvements during the last years [11,13]. SUMO is based on an airframe, which is a slightly modified version of the commercially produced model aircraft FunJet (Multiplex), and the Paparazzi autopilot system, an open source project under guidance by the École Nationale de l'Aviation Civile (ENAC) in Toulouse, France [14]. The autopilot system relies on attitude and position measurements obtained from an inertial measurement unit (IMU) and a GPS sensor, respectively.

In addition to the standard meteorological sensors for temperature, humidity and pressure, the SUMO system was equipped with fast-response sensors for the measurements of turbulent fluctuations in wind and temperature. The 3-dimensional flow vector was measured by a five-hole flow probe (5HP) with corresponding pressure transducers and data logger [10]. The probe was operated at a sampling rate of 100 *Hz*. By applying a coordinate transformation, accounting for the aircrafts attitude and position, the flow data in the reference system of the airplane can be converted into a meteorological coordinate system, from which turbulence quantities, such as the turbulent kinetic energy (TKE) can be obtained [15]. For the measurement of temperature fluctuations a fine-wire temperature (FWT) sensor, developed at the University of Tübingen [16], was operated at a sampling rate of 20 *Hz*. Both sensors were mounted at
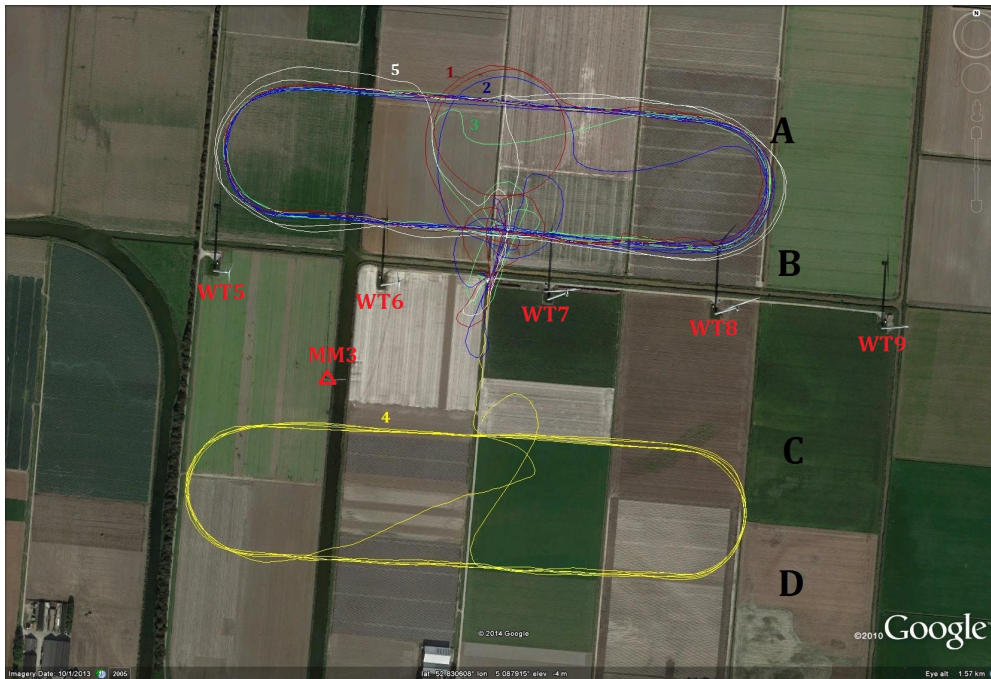
Fig. 2. Location of the 5 NORDEX N80 2.5 MW turbines (WT5-WT9) and the meteorological mast at the ECN test site Wieringermeer, together with the flight tracks of the 5 SUMO flights performed on May 10, 2014. The wind was coming from Southwest, placing the flights # 1-3 and 5 downstream and the flight # 4 upstream the row of wind turbines.

the nose of the SUMO aircraft as shown in Fig. 1. The FWT was only operated for experimental purposes and got in addition damaged during the landing of flight # 1. The corresponding data are not taken into account for the analysis presented here.

3. Measurements

3.1. Measurement campaign

The SUMO flights presented in this study were embedded in the joint measurement campaign WINTWEX-W [17], performed in collaboration between NORCOWE and the Energy Center of the Netherlands (ECN). This campaign was specifically dedicated to the full-scale investigation of structure and dynamics of single turbine wakes and lasted from November 2013 to May 2014 at the ECN test site Wieringermeer in the Netherlands. The main purpose of the campaign was the qualitative and quantitative description of single wind turbine wakes with respect to structure, propagation and persistency under various atmospheric conditions. The infrastructure of the test site relevant for this study consists mainly of a nearly East-West oriented row of five Nordex N80 2.5 MW research wind turbines (WT5-WT9 in Fig. 2), with a hub height and rotor diameter (D) of 80 *m*. A meteorological mast (MM3 in Fig. 2) is located approximately 3 D upstream of WT6 for the main wind direction from Southwest.

In addition to the permanently operated meteorological mast, equipped with cup and sonic anemometers, several wind lidar systems have been deployed during WINTWEX-W [17]. For the characterization of the inflow, the 108 *m* mast measurements were complemented by a static lidar wind profiler (Leosphere WindCube v1) and a forward-looking nacelle mounted lidar (Avent Wind Iris) on WT6. For the wake investigations one scanning wind lidar system (Leosphere 100S) was located ca. 12 D downstream WT6 in the main wind direction. It was scanning every minute a pattern consisting of three horizontal Plan Position Indicator (PPI) scans of 60 *deg* at elevations of 2.4, 4.7 and 7.1 *deg* and three vertical Range Height Indicator (RHI) scans of 60 *deg* at a fixed azimuth direction of 228 *deg* pointing towards WT6. Additional static wind profilers (Leosphere WindCube v1) measured wind profiles every
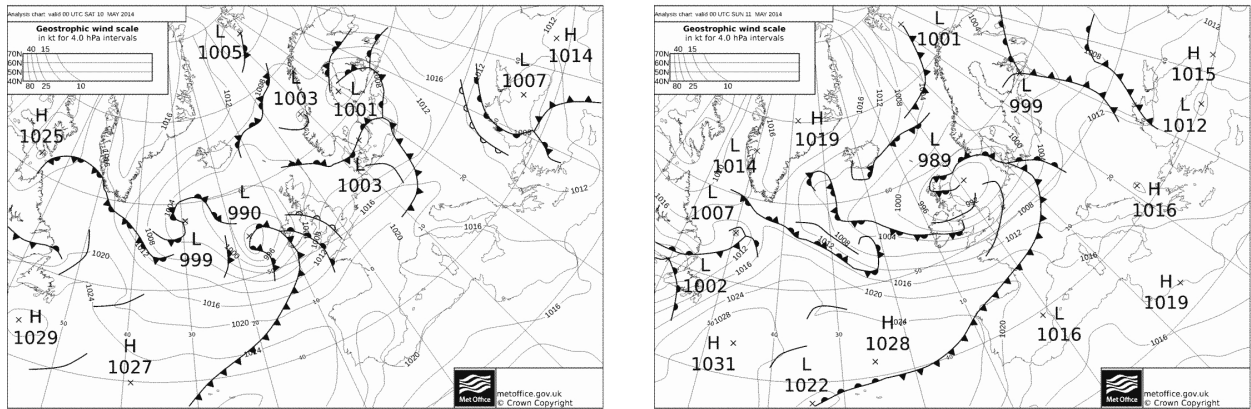
Fig. 3. Surface analysis showing isobars and fronts for the 10.05.2014 0 UTC (left) and 11.05.2014 0 UTC (right). The charts are provided by the UK Meteorological Office and have been downloaded from http://www.wetterzentrale.de/topkarten/tkfaxbraar.htm.

second at a distance of 1.75 and 3.25 D downstream of WT6. During parts of the campaign this turbine has also been equipped with a downstream-looking nacelle lidar (ZephIR 300), complementing the wake measurements by the static and scanning lidar systems described above. A detailed description of the campaign and the instrumentation and scan patterns can be found in [17].

3.2. SUMO operations

The general synoptic situation on May 10, 2014 was characterized by considerable low pressure activity in the North Atlantic region transporting frontal systems and relatively moist air masses in a mostly westerly flow towards Europe (see Fig. 3). A frontal passage during the night and morning of May 10 was accompanied by nearly continuous precipitation lasting until early afternoon. Around 13 UTC, the area got under the influence of a weak high pressure ridge, leading to a break in precipitation and a considerable decrease in cloudiness, opening a window of several hours suitable for SUMO operations. During this period Southwesterly wind of around 15 ms^{-1} were prevailing (see the horizontal wind speed v_h presented in panel 3 of Fig. 4). Due to the continuous increase in wind speed after the frontal passage, the SUMO operations had to be terminated at around 15:30 UTC. At that time the wind and turbulence conditions close to the ground got too risky for a safe landing of the SUMO system on the available landing ground. For the flights itself the ambient average wind speed of around 15 ms^{-1} with gusts up to 20 ms^{-1} did not pose any problems for the SUMO system. The tracks of the five flights performed are shown in Fig. 2 and corresponding key information is summarized in Table 1.

Table 1. SUMO flights performed on May 10, 2014.

flight #	start time [UTC]	# of legs	altitude [m]	position
1	13:55	4	120	A and B, downstream
2	14:08	10	80	A and B, downstream
3	14:30	4	120	A and B, downstream
	14:35	2	80	A and B, downstream
4	14:50	4	120	C and D, upstream
	14:56	4	80	C and D, upstream
5	15:14	3	120	A and B, downstream

4. Results

4.1. Comparison between SUMO 5HP and sonic anemometer

Figure 4 presents a comparison of wind speed measurements by SUMO (from flight # 4) and the sonic anemometer at 108 *m* on the meteorological mast. Both data sets represent upstream wind conditions. The presented sonic anemometer measurements cover the whole day of May 10. The 32 *Hz* data are plotted in black, the gray line denotes a 10 *min* running mean. The SUMO measurements are given as average values over each straight leg, resulting in a total of eight points (orange stars) for flight # 4. The panels show, from top to bottom, the East-West wind component *u*, the North-South wind component *v*, the horizontal wind speed v_h, and the vertical wind speed *w*. It can be seen that there is an excellent agreement for the *u* component between all eight SUMO legs and the sonic average. For the *v* component the SUMO measurements show a systematic underestimation of about 1.5 ms^{-1}. This is most likely caused by the fact that SUMO was flying with a yaw offset with respect to the flight direction, which was not measured and therefore had to be estimated. Uncertainties in this estimate could lead to the observed discrepancy [15]. The vertical component *w* from the SUMO measurements has a positive bias in the order of $1 ms^{-1}$. This is the result of a non-perfect horizontal positioning of the 5HP during the flight leading to a systematic, small offset in the angle of attack of the flow probe. It should, however, be mentioned that these systematic deviations in *v* and *w* will not affect the calculation of TKE presented in Section 4.2, as they are based on variances, i.e. the deviation from the mean, and not the mean itself.

A comparison of the spectral characteristics of the 100 *Hz* measurements from the 5HP of SUMO and the 32 *Hz* data from the sonic anemometer is presented in Fig. 5 for the example of leg 2 during flight # 4, performed around 14.52 UTC. It shows the instantaneous (left) and averaged (right) energy spectra of the wind velocity components *u*, *v*, and *w* (from top to bottom). In general both systems agree reasonably well and show a clear inertial subrange. The SUMO spectra show an increase in energy towards the highest frequencies. This is an indication of an aliasing effect close to the Nyquist-frequency of the 5HP of 50 *Hz*. The spectra for *u* agree very well over the inertial subrange. The only deviation is a slightly enhanced level of energy for the SUMO data around 1 *Hz*. SUMO movements, triggered by the internal control loops of the autopilot system, are the most likely cause of this enhancement. The spectra for three different averaging periods for the sonic data (2, 4 and 10 *min*) show that the choice of the averaging period does not affect the spectra in the inertial subrange for the conditions during the flight presented here. The peak around 1 *Hz* is also evident in the SUMO spectra for *v*. In this component there also seems to be a lack of energy in the SUMO data for the lower frequencies, a feature that requires further investigations. For the vertical component the SUMO and sonic spectra are again in good agreement over a wide range of frequencies. The SUMO data are following the -5/3 slope of the inertial subrange also for the highest frequencies, while the sonic data are showing signs of spectral attenuation in this region. This might be a signature of flow distortion by the mast. However, one single case should not be overinterpreted in this context. A more detailed analysis of these spectra is on its way and beyond the scope of this proof of concept study.

4.2. Wake characterization

Figure 6 presents the values of the East-West wind component *u* along the flight track given in UTM coordinates for the positions B (ca. 1.5 rotor diameters downstream) and D (upstream). The overall length of the x-axis presented is 1 *km* and the ticks are labeled every 100 *m*, i.e. the straight legs of the racetrack pattern used for these evaluation have a length of around 800 *m*. The thin gray lines show the data from the individual legs (10 in the case of B and 4 in the case of D). The data set presented in the upper panel for position B has been collected during the flights # 1-3 between 13:55 and 14:45 UTC, and the one in the lower panel for position D during flight # 4 between 14:50 and 15:05 UTC. The data from flight # 5 have been omitted in this context, as the wind speed had suddenly increased by nearly 5 ms^{-1} compared to the downstream flights # 1-3.

The individual legs show a high inter-leg variability, while the bin average over all legs and over 10 *m* in the East-West UTM coordinates displays a rather homogeneous behavior, in particular for position B with the higher number of legs averaged. The average background level of the wind speed component *u* is around 8 ms^{-1} for both positions. In the flight legs at B the wind turbines WT6 and WT7 create a clear signature in the *u* wind component. The reduction in wind speed reaches a maximum of 3-4 ms^{-1} and the wake deficit extends over a horizontal distance of about 150 *m*.
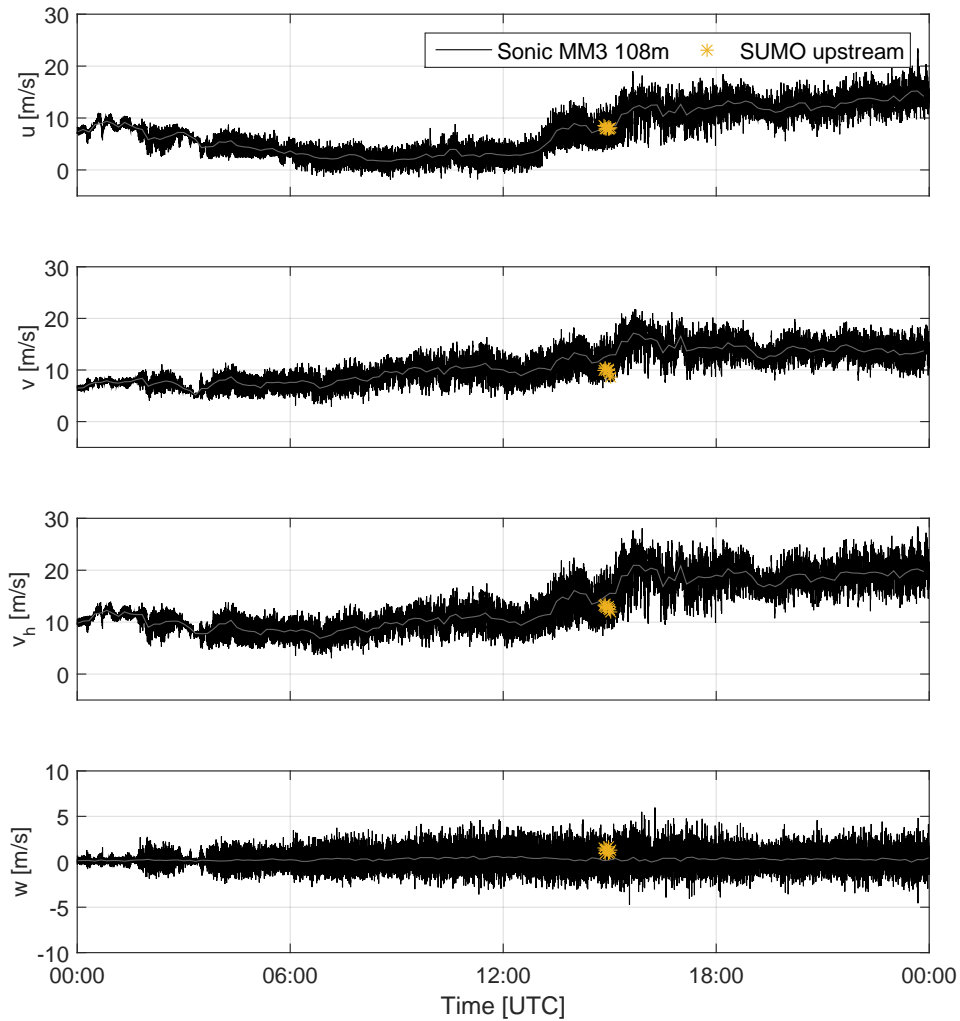
Fig. 4. Comparison of wind speed measurements taken by SUMO and the sonic anemometer at 108 *m* on the meteorological mast during flight # 4. The sonic anemometer data are given by the black lines, the SUMO data are marked by the orange stars. The panel show from top to bottom: East-West wind component *v*, North-South wind component *v*, horizontal wind speed v_h, and vertical wind speed *w*.

The wind speed deficit compares well to a deceleration of 3 ms^{-1} measured by the profiling lidar at 1.75 D under neutral conditions [17]. Also the horizontal expansion of the wake cone is comparable to results of horizontal PPI scans performed by the Wincube 100S, which show a wake width of around 120 *m*.

Figure 7 shows the TKE calculated from the velocity variances measured by SUMO as a function of the horizontal distance along the flight track for the 4 different positions with respect to the wind turbine row. Again the overall length of the x-axis presented is 1 *km* and the ticks are labeled every 100 *m*. The gray lines show the data from the individual legs. The thick colored lines indicate the average over all flight legs for each position (bin average over 10 *m* in East-west UTM coordinates). For positions A and B it is based on the data of 10 legs from flights # 1-3, for positions C and D on only 4 legs from flight # 4. Positions A and B show in general a distinct higher level of TKE and TKE variability compared to the upstream positions C and D. This is an indication of the turbulence induced by the wind turbine row. The prominent peak in the center of position C is based on the measurement of one single flight leg and could be either a measurement error or a real atmospheric signature caused by one of the five large
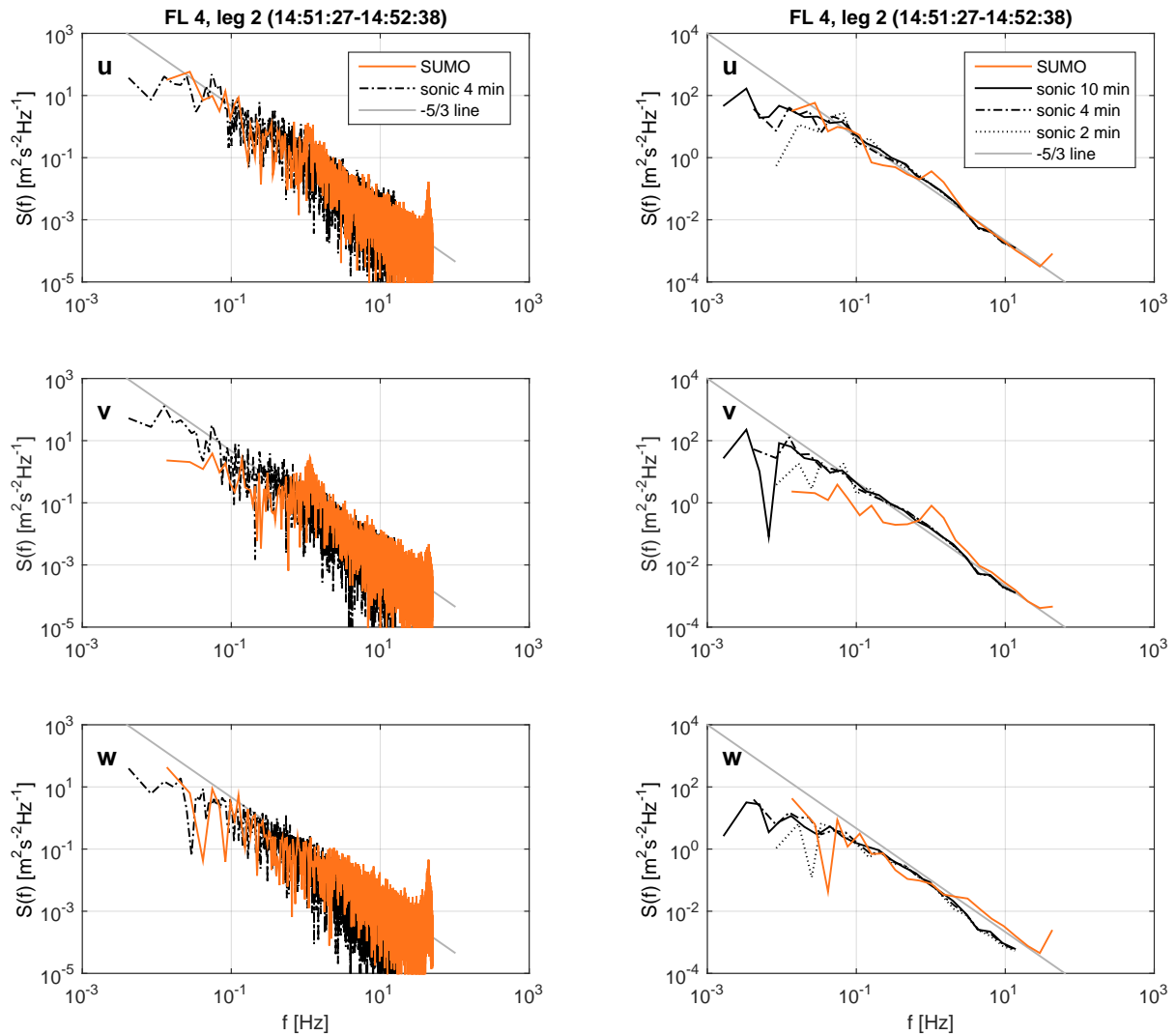
Fig. 5. Instantaneous (left) and averaged (right) energy spectra of the wind velocity components *u* (top), *v* (middle) and *w* (bottom) for leg 2 during flight # 4 at 14:52 UTC. The SUMO data are in orange, the sonic anemometer data in black. The gray lines indicate the expected -5/3 slope of the inertial subrange.

prototype turbines located ca. 1.5 *km* upstream the row of the test turbines investigated here. For position B (ca. 1.5 D downstream), we find the overall highest values, and we also see a clear signal from the individual wakes of the turbines WT5, WT6 and WT7, the one for WT5 only captured partially. The fully probed wakes of WT6 and WT7 show the highest TKE level in the flanks of the wake (indicated by the black arrows in the panel for B in Fig. 7), while the TKE in the center of the wake is only slightly enhanced compared to the background TKE. Again the wake deficit extends over a horizontal distance of about 150 *m*. For position A, at ca. 5 D downstream, we see no clear individual wake signals, at least not with the two-peak structure of position B, but in general an increased TKE level compared to the values in positions C and D.

5. Summary and Outlook

SUMO has been successfully operated in the vicinity of the five NORDEX N80 research turbines of the Energy Research Centre of the Netherlands (ECN) at the test site Wieringermeer and proven its capability for wind turbine
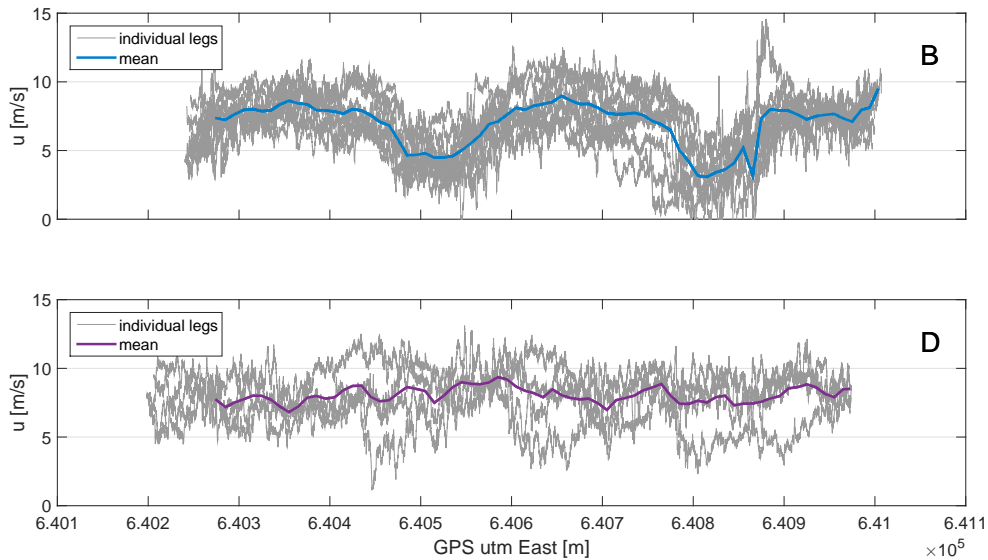
Fig. 6. East-West wind speed component u measured by SUMO in positions B (ca. 1.5 rotor diameter downstream the row of wind turbines) and position D (upstream). The thin gray lines show the data from the individual flight legs, the thick colored line in each plot indicates the average over all corresponding flight legs.

wake investigations. In rather high wind conditions of 15-20 ms^{-1} on May 10, 2014, the system showed a satisfying in-flight behavior and performed five flights for wind field and turbulence characterization also for situations above rated wind speed. A comparison of the wind measurements derived from the SUMO 5HP with observations from a sonic anemometer on a 108 *m* mast revealed an in general good agreement of the different systems, both in terms of average values and in the energy spectra derived from the time series. The values for the macrophysical wake parameters, as wake deficit of about 3 ms^{-1} and the horizontal wake extension of around 150 *m*, observed at flight legs 1.5 D downstream, are in excellent agreement with corresponding data from a scanning wind lidar system. In addition allow the SUMO measurements for a more detailed characterization of the TKE distribution across the wake, with the distinctly highest values in the flanks of the wake, most likely due to a combination of the turbulence directly induced by the tip vortices of the rotating turbine blades and additional TKE production in the outer shear zone of the wake. With that has SUMO clearly shown its potential of bridging and complementing mast and lidar measurements with respect to turbulence parameters and wake characteristics.

The results of the campaign presented here has also triggered the idea of new flight strategies for future measurement campaigns, e.g flying towards the wind turbine at different vertical levels and lateral displacement from the turbine centerline. This would result in rather low speed of SUMO over ground and therefore allowing to collect longer time series of the 3-dimensional flow vector for a given maximum length of flight legs, limited by the rules for Visual Line of Sight (VLOS) for RPAS operations. This would e.g. enable longer and more robust time series for spectral investigations, and a comparison of the turbulence structure inside and outside the wake affected air volume downstream.

A new dimension of wake measurements will in the future be opened by the combination of fixed-wing (e.g. SUMO) and rotary-wing RPAS. The latter will, due to their hovering capability, be able to perform longer time series at fixed, but freely selectable positions. Two corresponding quadcopter systems with turbulence measurement capacity have recently been purchased by the Geophysical Institute and are at the moment in the test and validation phase.
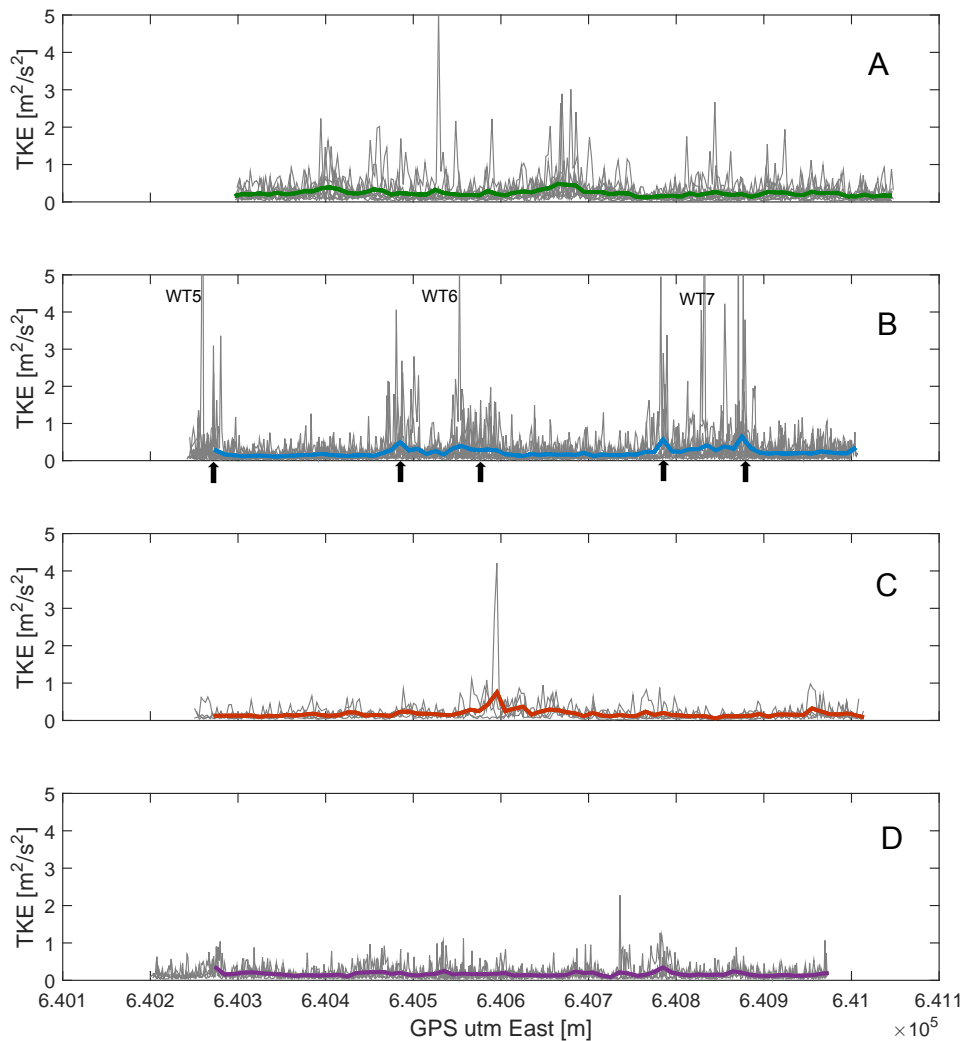
Acknowledgements

Fig. 7. TKE as function of the horizontal position as derived from the SUMO 5HP turbulence measurements for the 4 different positions with respect to the wind turbine row. The thin gray curves show the data from the individual flight legs, the thick colored line in each plot indicates the average over all corresponding flight legs.

References

[1] Barthelmie, R.J., Folkerts, L., Ormel, F.T., Sanderhoff, P., Eecen, P.J., Stobbe, O., et al. Offshore wind turbine wakes measured by sodar. Journal of Atmospheric and Oceanic Technology 2003;20(4):466–477. URL: ¡Go to ISI¿://000182107600004.

[2] Wharton, S., Lundquist, J.K.. Assessing atmospheric stability and its impacts on rotor-disk wind characteristics at an onshore wind farm. Wind Energy 2012;15(4):525–546. doi:10.1002/we.483.

[3] Bingöl, F., Mann, J., Larsen, G.C.. Light detection and ranging measurements of wake dynamics part I: one-dimensional scanning. Wind Energy 2010;13(1):51–61. doi:10.1002/we.352.

[4] Aitken, M.L., Banta, R.M., Pichugina, Y.L., Lundquist, J.K.. Quantifying Wind Turbine Wake Characteristics from Scanning Remote Sensor Data. Journal of Atmospheric and Oceanic Technology 2014;31:765–787. doi:10.1175/JTECH-D-13-00104.1.

[5] Iungo, G.V., Porté-Agel, F.. Volumetric LiDAR scanning of wind turbine wakes under convective and neutral atmospheric stability regimes. Journal of Atmospheric and Oceanic Technology 2014;:140822100122000doi:10.1175/JTECH-D-13-00252.1.

[6] Elston, J., Argrow, B., Stachura, M., Weibel, D., Lawrence, D., Pope, D.. Overview of Small Fixed-Wing Unmanned Aircraft for Meteorological Sampling. Journal of Atmospheric and Oceanic Technology 2015;32(1):97–115. doi:10.1175/JTECH-D-13-00236.1.

[7] Wildmann, N., Hofsäß, M., Weimer, F., Joos, A., Bange, J.. MASC a small Remotely Piloted Aircraft (RPA) for wind energy research. Advances in Science and Research 2014;11:55–61. doi:10.5194/asr-11-55-2014.

[8] Kocer, G., Mansour, M., Chokani, N., Abhari, R., Müller, M.. Full-Scale Wind Turbine Near-Wake Measurements Using an Instrumented Uninhabited Aerial Vehicle. Journal of Solar Energy Engineering 2011;133(4):041011. doi:10.1115/1.4004707.

[9] Mansour, M., Kocer, G., Lenherr, C., Chokani, N., Abhari, R.S.. Seven-Sensor Fast-Response Probe for Full-Scale Wind Turbine Flowfield Measurements. Journal of Engineering for Gas Turbines and Power 2011;133(8):081601. doi:10.1115/1.4002781.

[10] Aeroprobe, . On-The-Fly! Air Data System Users Manual Revision F, 1/2012. 2012. https://recuv-ops.colorado.edu/.../OTF_Manual.pdf.

[11] Reuder, J., Jonassen, M.O., Ólafsson, H.. The Small Unmanned Meteorological Observer SUMO: Recent developments and applications of a micro-UAS for atmospheric boundary layer research. Acta Geophysica 2012;60(5):1454–1473. doi:10.2478/s11600-012-0042-8.

[12] Reuder, J., Brisset, P., Jonassen, M., Müller, M., Mayer, S.. The Small Unmanned Meteorological Observer SUMO: A new tool for atmospheric boundary layer research. Meteorologische Zeitschrift 2009;18(2):141–147. doi:10.1127/0941-2948/2009/0363.

[13] Reuder, J., Båserud, L., Jonassen, M.O., Kral, S., Müller, M.. Exploring the potential of the RPA system SUMO for multi-purpose boundary layer missions during the BLLAST campaign. Atmospheric Measurement Techniques Discussions 2015;.

[14] ENAC, . Paparazzi user's manual. 2008. http://paparazzi.enac.fr/wiki_images/Users_manual.pdf.

[15] Båserud, L., Reuder, J., Jonassen, M.O., Kral, S., Bakhoday Paskyabi, M., Lothon, M.. Proof of concept for turbulence measurements with the RPAS SUMO during the BLLAST campaign. Atmospheric Measurement Techniques Discussions 2015;.

[16] Wildmann, N., Mauz, M., Bange, J.. Two fast temperature sensors for probing of the atmospheric boundary layer using small remotely piloted aircraft (RPA). Atmospheric Measurement Techniques 2013;6(8):2101–2113. doi:10.5194/amt-6-2101-2013.

[17] Kumer, V.M., Reuder, J., Svardal, B., Sætre, C., Eecen, P.. Characterisation of Single Wind Turbine Wakes with Static and Scanning WINTWEX-W LiDAR Data. Energy Procedia 2015;80(1876):245–254. doi:10.1016/j.egypro.2015.11.428.